scientific reports

Check for updates

OPEN

Unveiling the link between oversizing ratio and neointimal hyperplasia in a porcine model

Maofeng Gong, Rui Jiang, Xu He & Jianping Gu✉

Intimal hyperplasia (IH) is a major risk for inferior vena cava (IVC) filter retrieval failures and potentially fatal vascular trauma to the IVC or caudal vena cava (CVC) wall post-retrieval. However, demonstrating neointimal formation in humans presents challenges due to the difficulty in obtaining quantitative pathological evidence from the IVC. Here, it was hypothesized that the mismatch between the diameter of the CVC and the filter would correlate with increased IH. Radial force (RF) exerted by filter struts at various CVC diameters was tested in vitro. In vivo, Bama miniature swine were randomly fitted with IVC filters of 32 mm–20 mm diameter, and a three-dimensional digital subtraction angiography model was used to determine the oversizing ratio (OR). After dwelling times of 2, 3, and 4 weeks, the macroscopic CVC wall and intima in the areas adjacent to IVC filter struts were observed. The proliferation and thickness of IH and presentations of vascular smooth muscle cells (VSMCs) were evaluated. Masson trichrome staining was used to determine the production of collagen fiber. The RFs of the IVC filter consistently increased with the OR, suggesting a correlation coefficient ($R^2 = 0.74$, $p < 0.001$). Notable response in the CVC wall after filter placement, characterized by vessel wall injury, VSMCs dedifferentiation, proliferation, and extracellular matrix secretion, which tended to increase and change over time. Increased ORs and dwelling time correlated linearly with greater IH thickness (adjusted $R^2 = 0.456$, $p < 0.001$). Moreover, restricted cubic splines (RCS) analysis revealed that ORs had a non-linear relationship with the IH thickness after adjusting for the IVC filter dwelling time (nonlinear $p = 0.047$, $p < 0.001$). A linear correlation was also noted between increased ORs and dwelling time with the collagen area fraction (adjusted $R^2 = 0.860$, $p < 0.001$). Furthermore, RCS indicated a consistently higher risk of increased collagen fiber content when the OR exceeded 100.75% (nonlinear $p = 0.047$, $p < 0.001$). IH developed in response to CVC injury, VSMCs proliferation, and secretion of the extracellular matrix collagen fiber. RFs increased with increased ORs. Increased ORs and dwelling time correlate linearly with greater IH thickness and increased production of collagen fiber.

Keywords Intimal hyperplasia, Proliferation, Radial force, Porcine model, Oversizing ratio

Abbreviations

CVC	Caudal vena cava
IVC	Inferior vena cava
IVCF	Inferior vena cava filter
IH	Intimal hyperplasia
RF	Radial force
OR	Oversizing ratio
DVT	Deep vein thrombosis
PE	Pulmonary embolism
VSMCs	Vascular smooth muscle cells
DSA	Digital subtraction angiography
SD	Standard deviation

The recent few decades have seen the utilization of inferior vena cava filter (IVCF) rush into the forefront of clinical practice. Since its first introduction[1], the IVCF, a mechanical device, has been implemented to prevent fatal pulmonary embolism (PE) in patients with deep vein thrombosis (DVT) who are unable to receive appropriate therapeutic anticoagulation therapy or have failed standard therapy[2–4]. However, many

Department of Interventional and Vascular Radiology, Nanjing First Hospital, Nanjing Medical University, Nanjing 210006, Jiangsu, People's Republic of China. ✉email: gujianpingnj@163.com

controversies surrounding its use and net benefit remain because it does not come without risks, short- or long-term complications such as IVCF migration (< 1%), fractures (2–10%), thrombosis (1.6–33%), inferior vena cava (IVC) wall perforation (0–41%), and IVC occlusion have gradually been reported in the literature[2–8]. Hence, it is strongly recommended to retrieve the IVCFs whenever possible[5,6]. However, the challenge, and sometimes the impossibility, of retrieval remains a significant concern with IVCF. The overgrowth of cava vena intimal hyperplasia (IH) has been linked to failures in filter retrieval and potentially fatal vascular trauma to IVC wall post-retrieval[7–9].

The underlying pathophysiological process of IH in IVC, which is named as caudal vena cava (CVC) in swine, following IVCF placement has been addressed. Thors et al.[8] identified a significant response in the CVC wall 6th weeks after the IVCF placement, characterized by pronounced collagen deposition in trichrome staining. The intima and media layers were found to be 2–3 times thicker than normal in 90% of the subjects. Beginning on the 20th day post-placement, signs of fibrosis were noted, marked by thick IH and complete involvement of the IVCF struts, which contributes to the difficulty in filter retrieval. Dowell et al.[9] and our previous study[10] observed a trend of increasing radial force (RF) exerted by IVCF struts and a gradual narrowing of the IVC diameter in patients post-IVCF placement depicted on CT follow-ups. Our previous studies[5,6,11,12] also found a close relationship between the mismatch of IVC and IVCF diameters and IVCF-related thrombosis. These findings implied the importance of considering the compatibility and reactivity between IVCF and IVC diameters as well as the dwelling time. Despite these insights, there remains currently an overall paucity of what extent a diameter mismatch contributes to the IH of the vena cava wall.

We hypothesized that an appropriate oversizing ratio (OR)-where the diameter of the IVCF exceeds that of the IVC or CVC-is crucial to ensure stability and prevent IVCF migration. However, an excessive OR may accelerate the development of IH, rendering early IVCF removal potentially detrimental to the IVC or CVC, while prolonged retention could lead to IVC or CVC occlusion[5,13]. We wonder whether the use of IVCF with varying ORs and dwelling time could serve as an available strategy to mitigate IH. Therefore, the purpose of this experimental study is to investigate the correlation among the OR, dwelling time, and IH, ultimately proposing OR recommendations for IVCF deployment. This OR seeks to balance the prevention of filter migration with the minimization of IH development. Furthermore, the study may provide a theoretical basis for the improvement and innovation of IVCF designs, facilitating the clinical implementation of personalized and precise IVCF use.

Materials and methods

Animals

All swine were purchased from the Laboratory Animal Center of Nanjing First Hospital. A total of twelve Bama miniature swine were included in the present study (six males, six females; aged 45–55 weeks; weighing 25–35 kg). This strain was selected primarily based on prior experience. These mature swines exhibit a stable physiological state, which helps minimize the potential impact of natural growth and development on the experimental results. Animals were randomly classified into two groups: Group A, which was modeled with a filter of 32 mm diameter, which is currently available for clinical use; and Group B, modeled with a filter of 20 mm diameter, representing a new design. This study was conducted in strict adherence to the Guideline for Care and Use of Laboratory Animals, and the protocol was approved by the Animal Ethics Committee of Nanjing First Hospital, Nanjing Medical University. All methods were performed in accordance with the relevant guidelines and regulations.

All swine were sedated with an intramuscular injection of ketamine hydrochloride (15 mg/kg) and atropine sulfate (0.04 mg/kg). Anesthesia was induced with an anesthesia machine (Rui Wode Life Science and Technology Co. Ltd, Shenzhen, China) using inhaled isoflurane (5%, 100 mL glass bottles, Rui Wode Life Science and Technology Co. Ltd, Shenzhen, China) administered by face mask. Anesthesia was maintained in general anesthesia with isoflurane (1.5–3%) and oxygen (0.8 L/min). All animals were monitored during the procedures.

Inferior vena cava filters manufacturing

Two different diameters of retrievable IVCF (Illicium, Visee Medical Instruments Co. Ltd, Shandong, China) were acquired from Visee Medical Instruments Company. The filter (55 mm in length) is crafted from a nickel-titanium alloy using laser engraving, featuring an integrated design. It has perfect biological adaptability and flexibility, as well as 6 longitudinal struts. The filter with a diameter of 32 mm ($\Phi = 32$ mm) is suitable for standard clinical applications, while that with a diameter of 20 mm ($\Phi = 20$ mm) is specifically designed for use in animal experiments (Fig. 1A,B). Each specification was implanted in a swine. Pre- and post-IVCF placement, digital subtraction angiography (DSA) was conducted in two projections to assess the patency and diameter of the CVC.

In vitro tests of radial force between the filter and CVC diameter, OR

RF was tested by a Radial Compression Station (Blockwise Engineering LLC, Tempe, AZ). Blockwise employs a linear relationship between the positions of the extension arm and the diameter of the compression station, as shown in Fig. 1C, D. The RFs of IVCFs with diameters of 32 mm, 28 mm (only for RF testing), and 20 mm were performed in the mimic CVCs with diameters of 5 mm, 10 mm, and 15 mm. Each measurement was repeated five times.

To conduct a more accurate measurement of vena cava diameter below the renal vein in swine, three-dimensional DSA imaging was utilized. This was followed using three-dimensional reconstruction images to determine a model with the optimal imaging angle for measuring the minimum and maximum CVC diameters (Fig. 1E–H). Notably, given that the shape of the CVC transformed into a circular form following IVCF

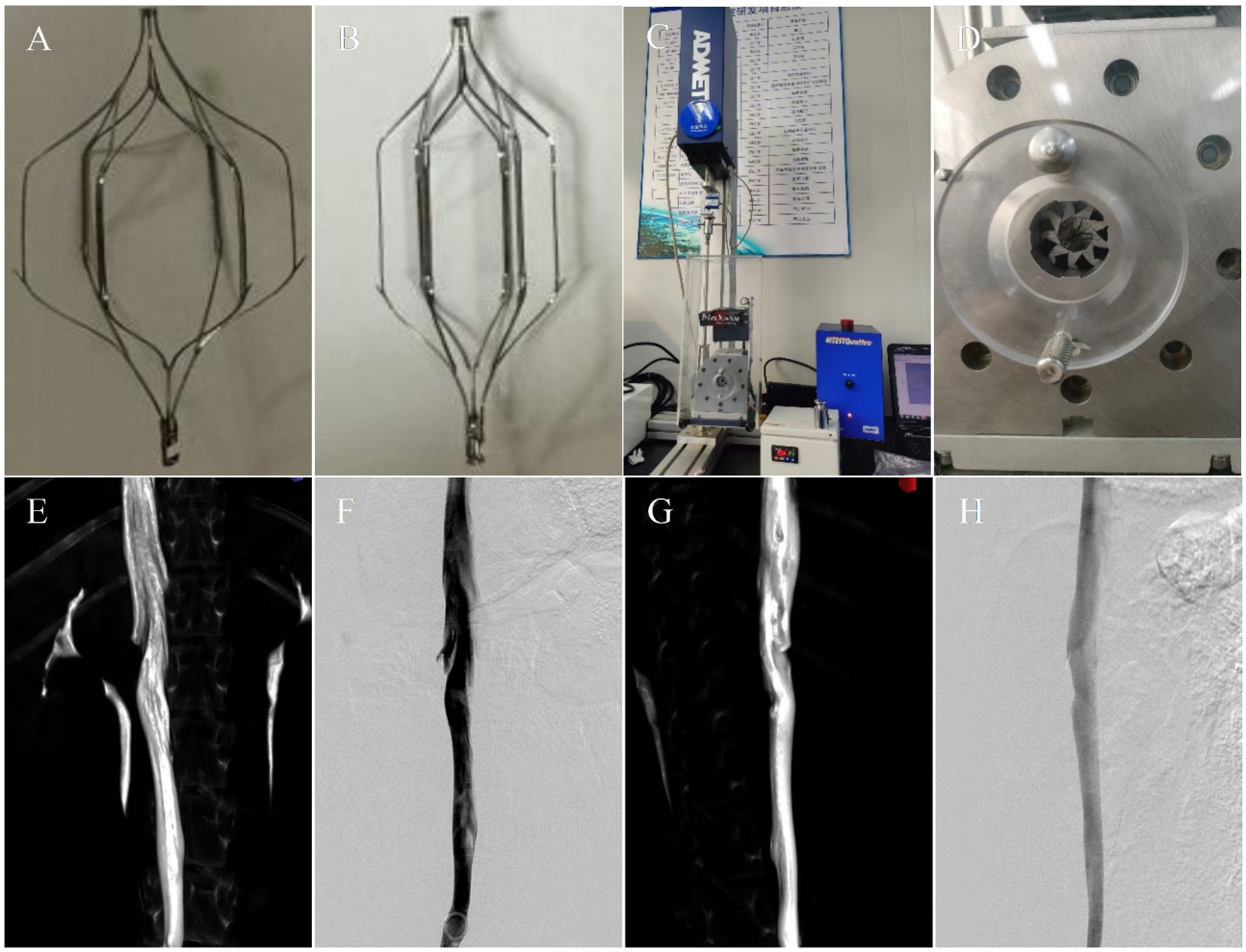

Fig. 1. A schematic representation of the spindle-shaped filter of 32 mm–20 mm diameter, radial force tests, and 3D-DSA imaging procedure. (**A**) Filter of 32 mm diameter. (**B**) Filter of 20 mm diameter. (**C**,**D**) In vitro tests of radial force conducted by a Radial Compression Station. (**E**–**H**) Utilization of three-dimensional DSA imaging to determine the optimal angle for measuring the maximum and minimum CVC diameter. (**E**,**F**) Measurement of the maximum CVC diameter. (**G**,**H**) Measurement of the minimum CVC diameter. *CVC* caudal vena cava.

deployment[6], the formula for converting the diameter of the CVC was used. The circumference of an ellipse (1,2) can be calculated into circular diameter (3) using the following formula

$$L = 2 \times \pi \times b + 4 \times (a - b) \tag{1}$$

$$d = \frac{L}{\pi} \tag{2}$$

Finally, the parameters of the model can be simplified as

$$d = 2b + 4 \times \frac{(a - b)}{\pi} \tag{3}$$

where L is the circumference of CVC, a is the semi-major axis, and b is the semi-minor axis, d is the diameter of CVC.

Then, the OR could be calculated according to the following equation.

$$OR = \left(\frac{\text{IVCF diameter}}{\text{CVC diameter}} - 1\right) \times 100\% \tag{4}$$

Experimental design and procedures

Briefly, all interventional procedures were conducted under the aseptic conditions. To investigate the morphology and diameter of the CVC, as well as the positioning of the renal vein, imaging was performed using both anterior-

posterior and lateral positions, along with three-dimensional DSA images. These images were obtained using a pigtail catheter (Cordis) inserted via the right or left femoral vein, with the injection of a non-ionic contrast agent (Iodixanol, 370 mgI/mL, Bayer Schering Pharma, Germany) at a rate of 5.0 mL/s, administering a total volume of 15 mL for general DSA or 35 mL for three-dimensional DSA.

Before catheter deployment of IVCF, all swine received a bolus of heparin (50 units per kilogram). The establishment of each animal swine model was standardized in the supine position on a DSA table. Every IVCF deployment was introduced through either the right or left femoral vein, using a modified Seldinger technique. If difficulty is encountered during the puncture, a minor incision can be made to directly access the vein or use ultrasound guidance for venipuncture. The implantation set of the IVCF supplied by the filter release sheath was used for delivery. Under fluoroscopy guidance to confirm proper filter placement relative to the renal veins, the filters were released about 2 mm below the renal vein. If the filter exhibited a tilt exceeding 15°, it was repositioned and released again. Control cavography post-delivery was performed using the same placement set. In every swine, an antibiotic (cefradine; 10 mg/kg) was administered intramuscularly for 3 days postoperatively for antibiotic prophylaxis. 40 mg of low weight molecular heparin (Enoxaparin; Sanofi, Madrid, Spain) was administered every day as thrombosis prophylaxis.

Venography via the femoral vein was conducted on weeks 2, 3, and 4 to investigate the positioning of the filter and identify any potential complications. Images obtained during these sessions were archived for subsequent analysis and measurement purposes.

Tissue sampling and histological analysis

Two swine per group underwent euthanized through intravenous injection of 10% potassium chloride (0.5 mL/kg) and 2% lidocaine (5 mg/kg) at 2, 3, and 4 weeks following IVCF placement. The CVC was then excised during autopsy to procure the neointima for macroscopic examination of IH, assessment of IVCF struts adhesion to the intima, and evaluation of intimal response. Length of 5.5 cm tissue samples were extracted from regions distant from the placement site of each CVC. The excised CVCs were isolated and immediately fixed in formalin at 4 °C overnight, followed by rinsing with distilled water. Then, they were dehydrated with a series of graded alcohol solutions and embedded in paraffin. The blindness of pathology analysis was strictly abided by in this study, a professor, blinded to the details of animal randomization, IVCF diameter used, and follow-up protocols, reviewed all specimens and conducted the analyses.

Microscopic examination focused on evaluating the responses of the intima and wall of the CVC in the areas adjacent to the IVCF struts. One venous tissue cross-section across the IVCF strut for each swine, ranging from 3 to 5 μm in thickness, were routinely stained with hematoxylin and eosin (H&E) for microscopic examination. Tissue sections were analyzed at 20× magnification using pathological color image analysis software (version 2.4.0; 3D Histech Ltd. Budapest, Hungary), integrated with a microscopic imaging system. The thickness of IH was randomly measured 6 times from the intimal layer to the IVCF strut. Verhoeff-Van Gieson (VVG) staining (Elastin kit; Richard-Allan Scientific, Kalamazoo, MI) was used to visualize the elastin and collagen fiber architecture of CVC. The protocol is used for staining which shows elastin fibers as dark brown and collagen fibers as light red.

Masson trichrome staining was used to determine the production of collagen fiber, Masson staining for collagen fiber appeared as blue. Image analysis was conducted using Image J software (version 1.50; National Institutes of Health, Bethesda, MD; available at http://rsb.info.nih.gov/ij/index.html) on randomly chosen vessel fields from each section. Given the predominance of collagen fibers in the vascular wall, the collagen area fraction in the hyperplasia area between intimal layer and strut contact site was calculated to assess the fiber content. Five fields of view were randomly selected for each tissue section, and within each, five areas were identified for detailed analysis. The average collagen fiber content was measured to indicate the quantity of collagen fiber present in the tissue, where a higher value suggests a higher content of collagen fiber in the tissue, indicative of more significant collagen fiber changes.

Sample size and statistical analysis

A total of 12 animals were included, with six in each group. The sample size was determined by budgetary constraints rather than a statistical model based on sample size calculations or expected outcomes. Data from this study was analyzed using the SPSS statistical software package (version 22.0; SPSS statistical software, Chicago, Illinois, USA) and R statistical language soft-ware (version 4.2.3; R Foundation, Vienna, Austria). Continuous variables following a normal distribution were presented as mean ± standard deviation (SD). For assessing the correlations among numerical variables, a student's t-test was used while assessing the correlation for numerical variables, as appropriate. Categorical variables were expressed as counts (percentage), with significance determined using the Chi-square test. Columns were generated with GraphPad Prism (9.0v; GraphPad Software Inc, CA, USA). Multiple linear regression analyses were performed with β, adjusted β, and 95% confidence interval (CI) to ascertain the association between OR, dwelling time, and IH. Restricted cubic splines (RCS) were utilized to model the dose-response relationship between OR and IH thickness or collagen fiber content flexibly, and a likelihood ratio test was applied to evaluate potential non-linearity. Statistical significance was considered based on a p-value < 0.050 (two-tailed).

Results

Animals baseline characteristics

In this study, a total of 12 swine were included for analysis, the mean age and weight in the two groups were 48.67 ± 1.63 weeks vs. 48.67 ± 1.50 weeks ($p = 1.000$) and 30.17 ± 0.68 kg vs. 30.25 ± 0.88 kg ($p = 0.86$). The detailed information has been shown in Table 1. No swine died or experienced procedure-related complications, such as major bleeding or infection during the study period. Technical success of the IVCF placement models was

Characteristic	All animals ($n=12$)	IVC filter with 32 mm diameter ($n=6$)	IVC filter with 20 mm diameter ($n=6$)	p-value
Demographics				
Age, weeks, mean ± SD	48.67 ± 1.50	48.67 ± 1.63	48.67 ± 1.50	1.000
Gender, male, n (%)	6 (50%)	3 (50%)	3 (50%)	1.000
Weight, kg, mean ± SD	30.21 ± 0.75	30.17 ± 0.68	30.25 ± 0.88	0.858
CVC diameter, mm, mean ± SD				
Maximum diameter	15.52 ± 3.06	16.51 ± 3.23	14.53 ± 2.80	0.280
Minimum diameter	8.92 ± 2.07	8.80 ± 1.86	9.03 ± 2.44	0.861
[†]Modeled diameter	13.12 ± 2.05	13.72 ± 2.01	12.53 ± 2.08	0.338
OR, %, mean ± SD	100.75 ± 50.38	137.93 ± 38.08	63.56 ± 28.55	0.003
IH thickness, μm, mean ± SD				
At 2nd week	245.73 ± 156.00	364.91 ± 137.21	126.55 ± 32.72	< 0.001
At 3rd week	541.62 ± 388.17	786.76 ± 420.30	296.48 ± 85.34	0.001
At 4th week	671.00 ± 323.45	845.67 ± 340.06	496.33 ± 191.16	0.005
Collagen area fraction, %, mean ± SD				
At 2nd week	12.03 ± 3.55	14.71 ± 2.94	9.34 ± 1.41	< 0.001
At 3rd week	26.64 ± 8.68	34.32 ± 4.76	18.96 ± 2.31	< 0.001
At 4th week	45.90 ± 15.33	59.35 ± 9.30	32.44 ± 2.66	< 0.001

Table 1. Baseline demographics, CVC diameter, OR, IH thickness, and collagen area fraction of the porcine model with various IVC filter diameters. *IVC* inferior vena cava, *CVC* caudal vena cava, *OR* oversizing ratio, *IH* intimal hyperplasia, *SD* standard deviation. [†]The morphology of the CVC transformed into a circular IVC following filter placement. Continuous data are presented as the means ± standard deviations; categorical data are given as the counts (percentage).

achieved in all swine (12/12). Overall, there was no difference in technical success rate, minor complications, or angiographic findings within each group. Angiography revealed no IVCF-related complications, such as angulation (> 15°), migration (> 10 mm), thrombosis, and penetration (> 3 mm).

In vitro tests of radial force between the IVCF and CVC diameter

The analysis demonstrated that the RFs of IVCF devices consistently increased as the diameter increased, with a correlation coefficient ($R^2 = 0.74$, $p < 0.001$). This relationship can be visualized in Fig. 2 and mathematically represented as follows:

$$\mathrm{RF}\ (\mathrm{N}) = 7.04 \times \mathrm{e}^{-3} \times \mathrm{OR}\ (\%) + 3.57 \tag{5}$$

Where RF represents the radial force (in Newtons (N)), and OR is the oversizing ratio (in %), demonstrating how the RF of the IVCF correlates with its size relative to the CVC diameter.

CVC morphology, magnification, and oversizing ratio

Angiography of the CVC prior to IVCF placement showed an oval shape with a mean anteroposterior maximum diameter of 15.52 ± 3.06 mm (range, 11.11–21.67 mm) and lateral minimum diameter of 8.92 ± 2.07 mm (range, 6.57–13.55 mm) at the intended site of IVCF deployment. Following the three-dimensional DSA image used, the mean maximum and minimum CVC diameters measured in group A were 16.51 ± 3.23 mm and 8.80 ± 1.86 mm, respectively, which were similar to those in group B of 14.53 ± 2.80 mm ($p = 0.280$) and 9.03 ± 2.44 mm ($p = 0.861$). Notably, given that the shape of the CVC transformed into a circular CVC post-filter placement, the mean CVC diameter post-filter placement was determined to be 13.72 ± 2.01 mm vs. 12.53 ± 2.08 mm ($p = 0.338$), illustrating the transition of the CVC's shape following the procedure. The mean OR of group A was 137.93 ± 38.08%, which was significantly higher than that of 63.56 ± 28.55% in group B ($p = 0.003$).

In vitro macroscopical characterization of CVC after IVCF placement

Macroscopic presentations of the retrieved filters in 2, 3, and 4 weeks were depicted in Fig. 3. These demonstrated the significant vessel response in the CVC wall after the IVCF placement, characterized by proliferation of the vessel wall, which tended to be increased and changed over time. IH was macroscopically observed in the CVC wall where the IVCF was placed, and the thickness of the vessel wall was found to be more obvious around the areas in contact with the IVCF strut. Beginning on the 3rd-week post-placement, signs of fibrosis were noted, marked by thick IH and complete involvement of the IVCF struts, The hyperplasia became thicker with the dwelling time of the IVCF. CVC walls fitted with a 32 mm IVCF seemed to exhibit macroscopic thicker walls compared to those treated with a 20 mm IVCF at the same intervals.

H&E examination analyses

H&E examination showed subintimal thickening that had embraced the IVCF strut; this subintimal thickening revealed hyperplasia and hypertrophy of the intimal layer, and a thin media and adventitia layer, mainly

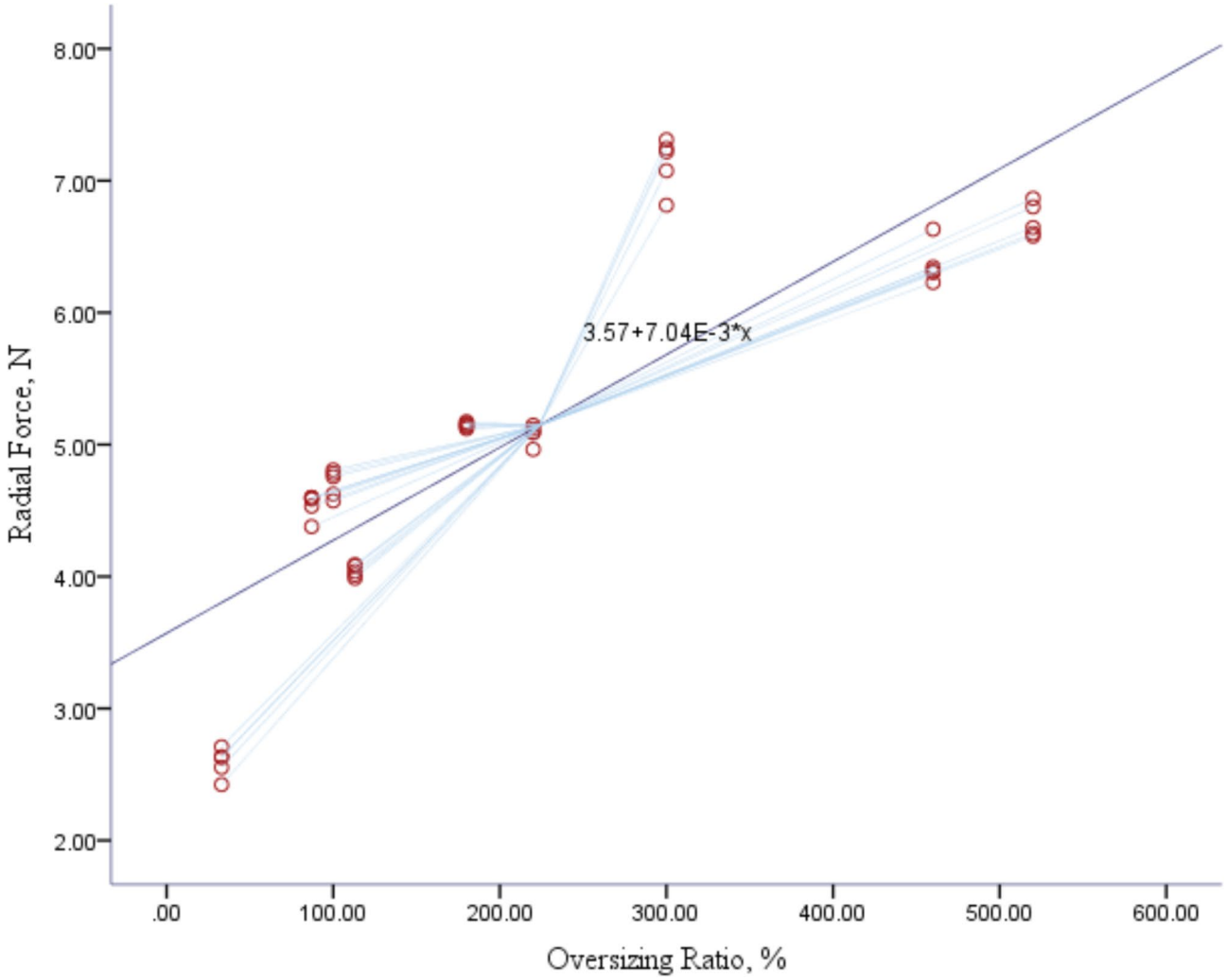

Fig. 2. RF increase correlates with OR. The relationship between the RFs of CVC filter devices can be mathematically represented as $\mathrm{RF}\ (\mathrm{N}) = 7.04 \times \mathrm{e}^{-3} \times \mathrm{OR}\ (\%) + 3.57$, suggesting that RFs consistently increased as the ORs increased, with a correlation coefficient ($R^2 = 0.74$, $p < 0.001$). *RF* radial force, *OR* oversizing ratio, *CVC* caudal vena cava.

secondary to the proliferation of non-striated muscle cells. As shown in Fig. 4, the thickness of the CVC wall was measured, IH thickness increased with the different filter diameters and dwelling time. The IVCF with a 32 mm diameter had a much higher IH thickness than the filter with 20 mm at the same intervals ($p < 0.05$), which implied that more severe IH was present following the increased OR. IH thickness was highly variable within and between OR at the follow-up time between 2, 3, and 4 weeks. To ascertain the association between OR, dwelling time, and IH thickness, multiple linear regression analyses (adjusted $R^2 = 0.456$, $p < 0.001$) were performed, which can be mathematically represented as follows.

$$\mathrm{IH\ thickness}\ (\mu\mathrm{m}) = 117.69 \times \mathrm{dwelling\ time}\ (\mathrm{weeks}) + 3.76 \times \mathrm{OR}\ (\%) - 245.86 \quad (6)$$

To control the factors of dwelling time, the relationship between IH thickness and OR was performed using the linear mixed models, there was a significant effect of OR on the thickness of IH ($F = 9.093$, df = 11, $p < 0.001$). Furthermore, this relationship was confirmed by RCS analysis by adjusting the confusing factor of dwelling time, which revealed a lateral S-shaped relationship between the risk of IH thickness and the OR (nonlinear $p = 0.047$), suggesting that an increased OR acted as a positive correlation with increased IH thickness when OR was larger than 100.75% (Supplementary Fig. 1. 1 A).

Verhoeff's Van Gieson stain, Masson staining analyses, and inflammation analyses

A thick CVC wall, generated beneath the lumen after IVCF placement, was light red on VVG staining (shown in Supplementary Fig. 2), demonstrating the extracellular matrix was mainly composed of collagen fibers, Masson stain was then analyzed. Presentations of Masson were similar to the H&E staining, the thickness of the vessel wall increased with the deposited collagen fibers following IVCF dwelling time. The normal three-layer structure

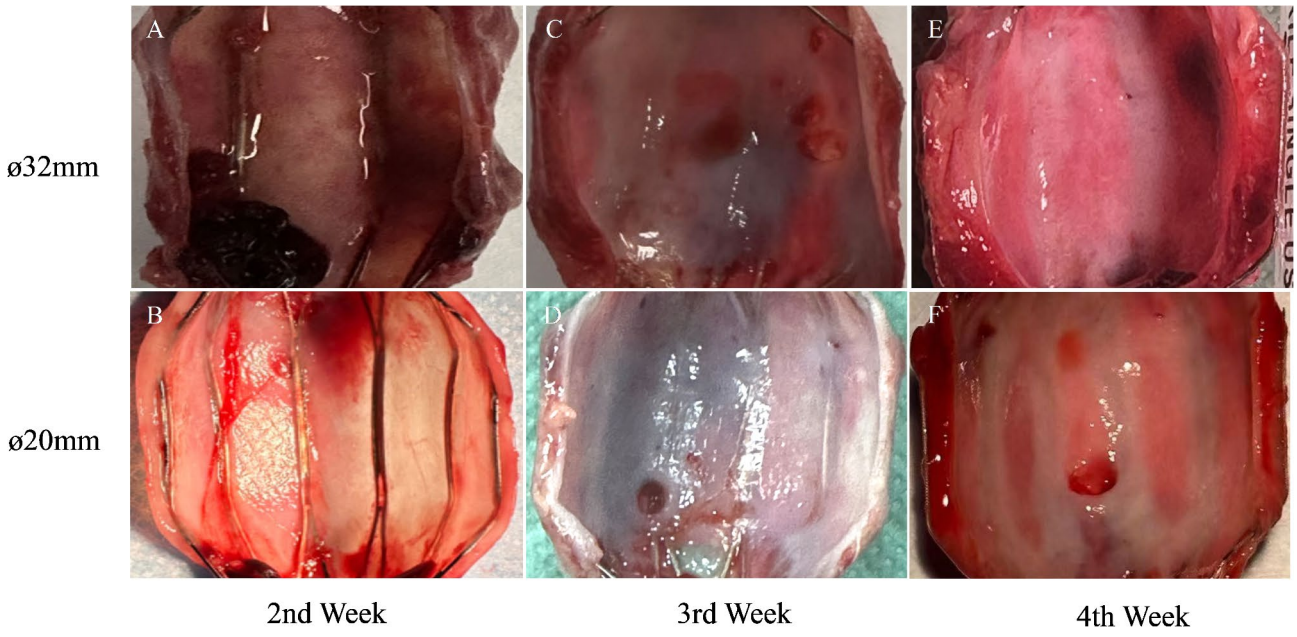

Fig. 3. Macroscopic presentations of the IVC filters in the 2nd, 3rd, and 4th week. (**A**–**F**) Demonstrates the significant vessel response in the CVC wall after the placement of filters with different diameters, characterized by the proliferation of the vessel wall, which tended to increase and change over time. At the same interval, IVC filter with a 32 mm diameter tended to have much higher macroscopic IH than filters with a 20 mm diameter. *CVC* caudal vena cava, *IH* intimal hyperplasia.

of vessel wall was disordered, the intima layer was markedly thickened, while the media and adventitia were thinned. The entire trajectory of the filter strut was covered by collagen fiber deposition, the image analysis revealed the semiquantitative results of collagen fiber content in the IVCF with two diameters (depicted in Fig. 5). The IVCF with a 32 mm diameter had a much higher collagen fiber content than the IVCF with 20 mm at the same follow-up time ($p < 0.05$), which implied that more severe collagen fibers were present following increased OR and dwelling time (adjusted $R^2 = 0.860$, $p < 0.001$). This relationship can be mathematically represented as follows.

$$\text{Collagen area fraction } \% = 12.32 \times \text{dwelling time (weeks)} + 0.18 \times \text{OR } (\%) - 27.20 \quad (7)$$

The correlations between collagen area fraction and OR were performed using the linear mixed models, suggesting a positive association between collagen area fraction % and OR following increased dwell time ($F = 183.08$, df = 11, $p < 0.001$). Moreover, this relationship was confirmed by RCS analysis, which revealed an inverted U-shaped relationship between the risk of collagen fibers and the OR (nonlinear $p < 0.001$), demonstrating that an increased OR acts as a risk factor for increased collagen fibers when OR was greater than 100.75% (**Supplementary Fig. 1**. 1B).

Discussion

This study presented a porcine model of the IH process in the vena cava in the presence of an IVCF, which mainly focused on CVC wall responses and biomechanical processes that occurred following spindle-shaped IVCFs with various ORs deployed. It captured key characteristics of the vessel wall process subjected to non-physiological mechanical forces over different times. In the in vitro study, we observed that the non-physiological mechanical forces—RFs—enlarged with the increased ORs of IVCF and CVC diameter. Further studies were carried out in vivo of swine among various ORs and dwelling time to investigate its possible correlations with IH thickness, suggesting that the increased ORs and dwelling time correlate linearly with greater IH proliferation. Moreover, RCS analysis revealed that ORs had a non-linear relationship with the IH thickness after adjusting for the IVCF dwelling time. Following the struts of IVCF were immersed in the CVC wall owing to myointimal remodeling, vascular smooth muscle cells (VSMCs) within the IH were hypothesized to undergo migration and phenotypic transformation from a contractile type to a synthetic state in response to the RFs activity. A linear correlation was also noted between the increased ORs and dwelling time with the collagen fibers content. Furthermore, RCS analysis indicated a consistently higher risk of increased collagen fiber content when the OR exceeded 100.75%.

Potential pathogenesis of CVC wall response after IVCF deployment with various ORs

The pathogenesis of CVC wall response following IVCF deployment with various ORs is still not well elucidated. The factors may be multifaceted and likely to have complex interactions in fostering this. Under different physiological conditions, mechanical forces such as cyclic stretch, pressure, and shear stress, are presumed to play fundamental roles in regulating the phenotypic transformation of VSMCs[14–16]. Jensen et al.[14] demonstrated

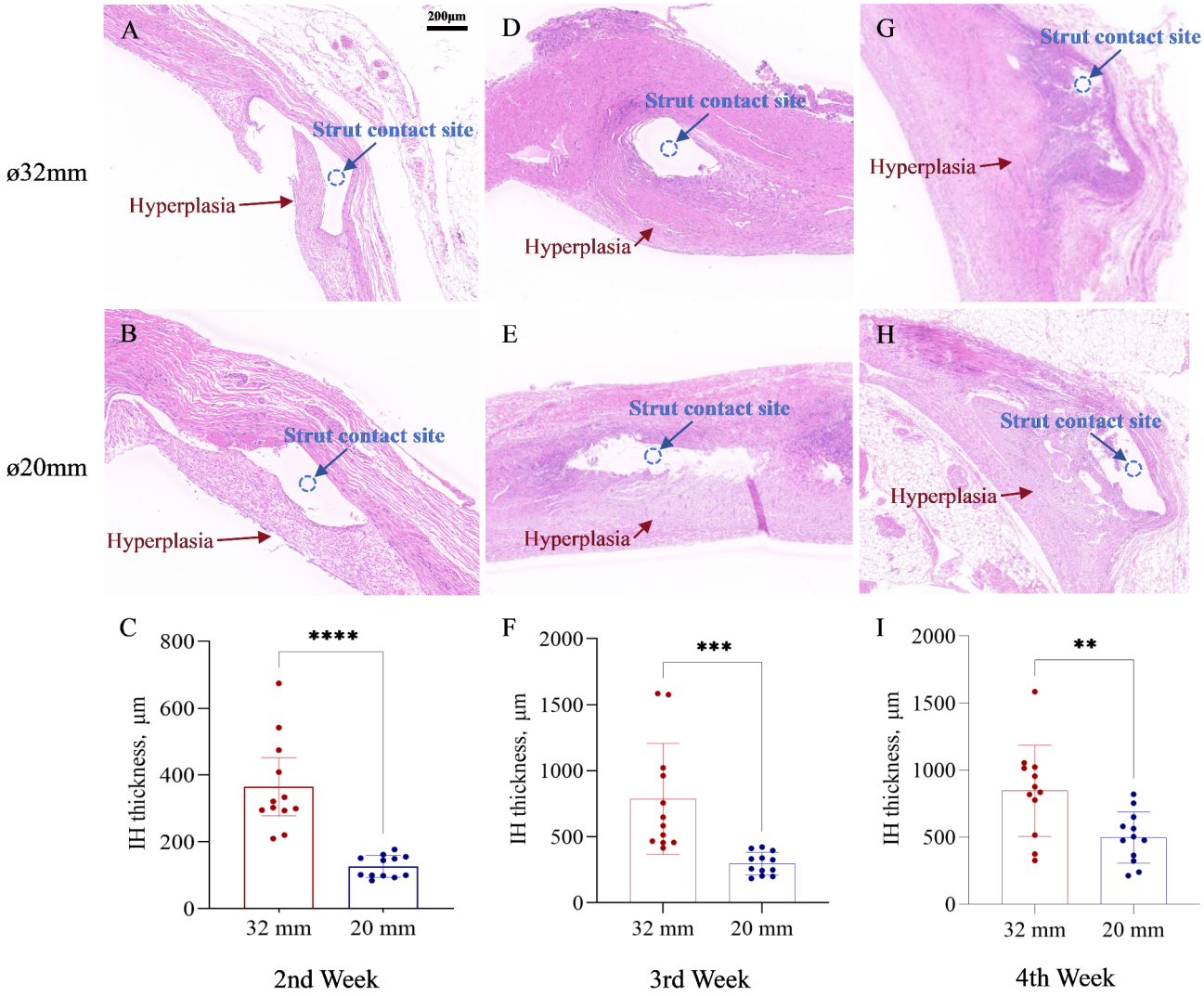

Fig. 4. Increased ORs increase IH thickness in the porcine model of filter placement on H&E stain, the image analysis revealed the semiquantitative results of IH thickness in the filter with two diameters. The IVC filter with a 32 mm diameter had a much higher IH thickness at the strut contact site than the filter with 20 mm. (**A**–**C**) At the 2nd week ($p < 0.0001$). (**D**–**F**) At the 3rd week. ($p < 0.001$). (**G**-**I**) At the 4th week ($p < 0.01$). *OR* oversizing ratio, *IVC* inferior vena cava, *IH* intimal hyperplasia.

that rat VSMCs, subjected to high tensile forces (> 10%) for 24 h, exhibit reduced expression of contractile markers such as calponin 1 and smoothelin, accompanied by an increase in the level of synthetic marker osteopontin, suggesting that high mechanical forces stimulation may induce the phenotypic transformation in VSMCs. Furthermore, Tang et al.[15] indicated that high mechanical tension can activate the ROCK/JNK/SP1 signaling pathway in VSMCs, leading to transcriptional repression of mitofusin 2 (MFN2). A deficiency in MFN2 can inhibit the ubiquitination and degradation of phosphofructokinase-1 (PFK1) mediated by the E3 ubiquitin ligase Tripartite motif-containing protein 21, thereby increasing the protein content of PFK1 and level of cellular glycolysis, resulting in the Warburg effect. These findings give us insights into understanding how changes in mechanical force impact the outcome of this process. In our study, it is hypothesized that the initial ORs affect the magnitude of RFs and that the RFs highly promote the VSMCs phenotypic transformation, enhance cell proliferation and migration, and determine the ultimate configuration of the tissue growth.

Our results suggested that the IH thickness varied from different ORs. The RFs were hypothesized to serve as the stimulus variable to start this process. The final distribution of IH is highly dependent on the endothelial denudation (stemming from RF activation); the migration of VSMCs into IH; the phenotypic transformation of synthetic VSMCs; and the synthesized collagen fiber (Fig. 6). The mean OR in swine that underwent an IVCF diameter of 32 mm was higher than that in swine with 20 mm. Moreover, RFs increased following the increased ORs, and a linear relationship between RFs and ORs was noted. Various ORs can induce distinct mechanical alterations, prompting varied responses in VSMCs subjected to different mechanical environments. Hence, the VSMC phenotypic alteration from contractile to synthetic type, proliferation, migration, and secretion were significantly enhanced. Thereby, triggering off the collagen fiber content, which was found the IVCF with a

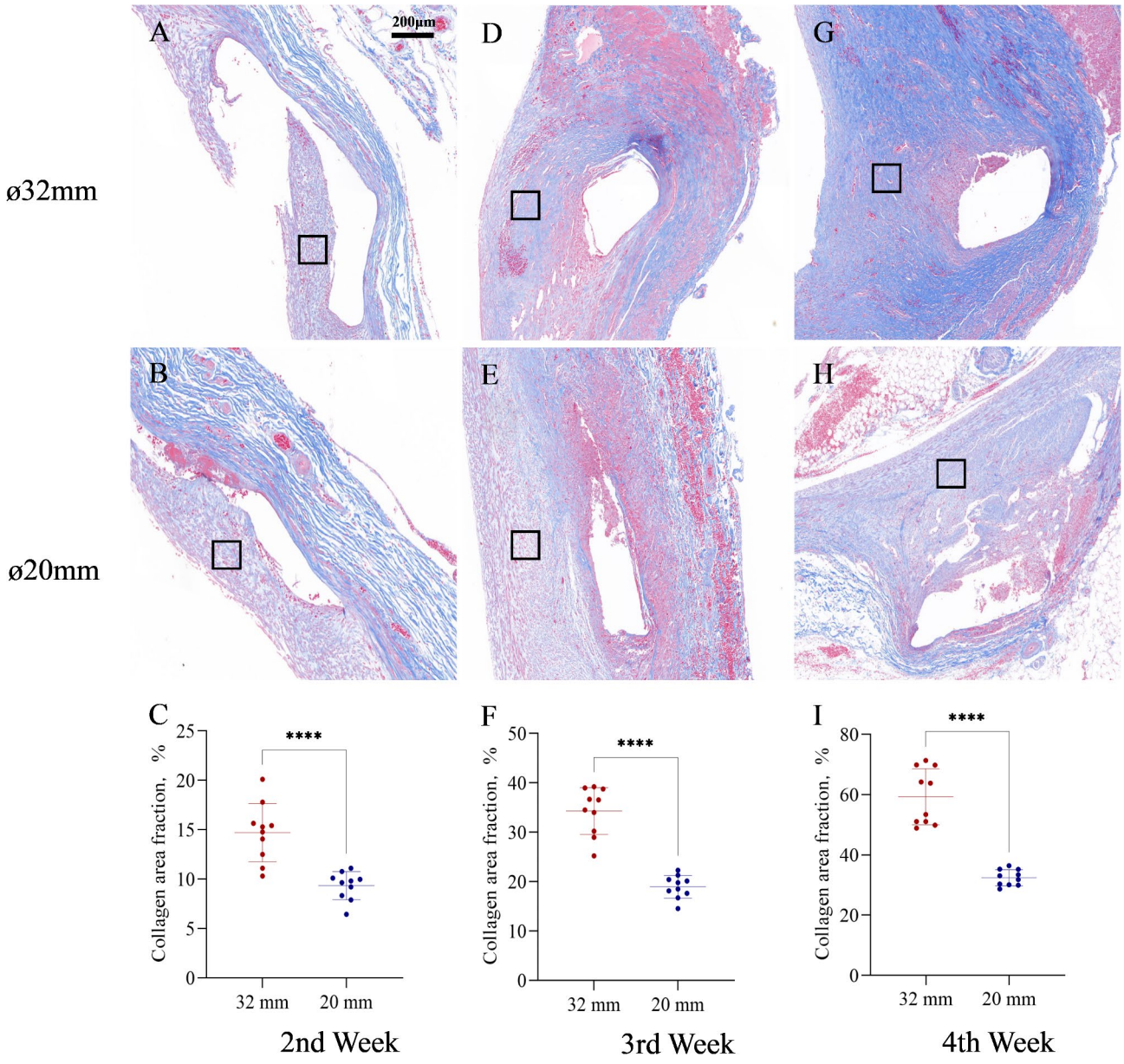

Fig. 5. Increased ORs increase collagen fiber in the porcine model of filter placement on Masson stain. The entire trajectory of the filter strut was covered by collagen fiber deposition. Image analysis revealed the semiquantitative results of collagen fiber content in filters with two diameters. The IVC filter with a 32 mm diameter exhibited a significantly higher collagen area fraction than the filter with 20 mm diameter. (**A**–**C**) At the 2nd week ($p < 0.0001$). (**D**–**F**) At the 3rd week. ($p < 0.0001$). (**G-I**) At the 4th week. ($p < 0.0001$). *OR* oversizing ratio, *IVC* inferior vena cava, *IH* intimal hyperplasia.

32 mm diameter had a much higher collagen fiber content than the IVCF with 20 mm at the same follow-up time ($p < 0.05$). These mechanisms were responsible for tissue growth. However, our study is limited by the lack of more in-depth genomic-level investigations.

Clinical implications of this study

The excessive IH following IVCF deployment may exert some adverse implications, IVCF retrieval is imperative to reduce risks of long-term complications[17]. For a start, removing the filter beyond the optimal time window, in addition to IH and inflammation in the cava wall[18], may ramp up the retrieval difficulty, thereby raising the likelihood of procedure-related complications, such as cava intima tearing and rupture bleeding. Moreover, prolonged retention of the IVCF can trigger luminal contraction and may even give rise to IVC or CVC obstruction[10]. Hence, minimizing the vessel responses would potentially improve retrieval and reduce the risks caused by long-term placement. Exploration of efficient therapy methods necessitates studies on minimizing the IH in IVC or CVC induced by IVCF. It is crucial to determine an appropriate IVCF/CVC diameter ratio,

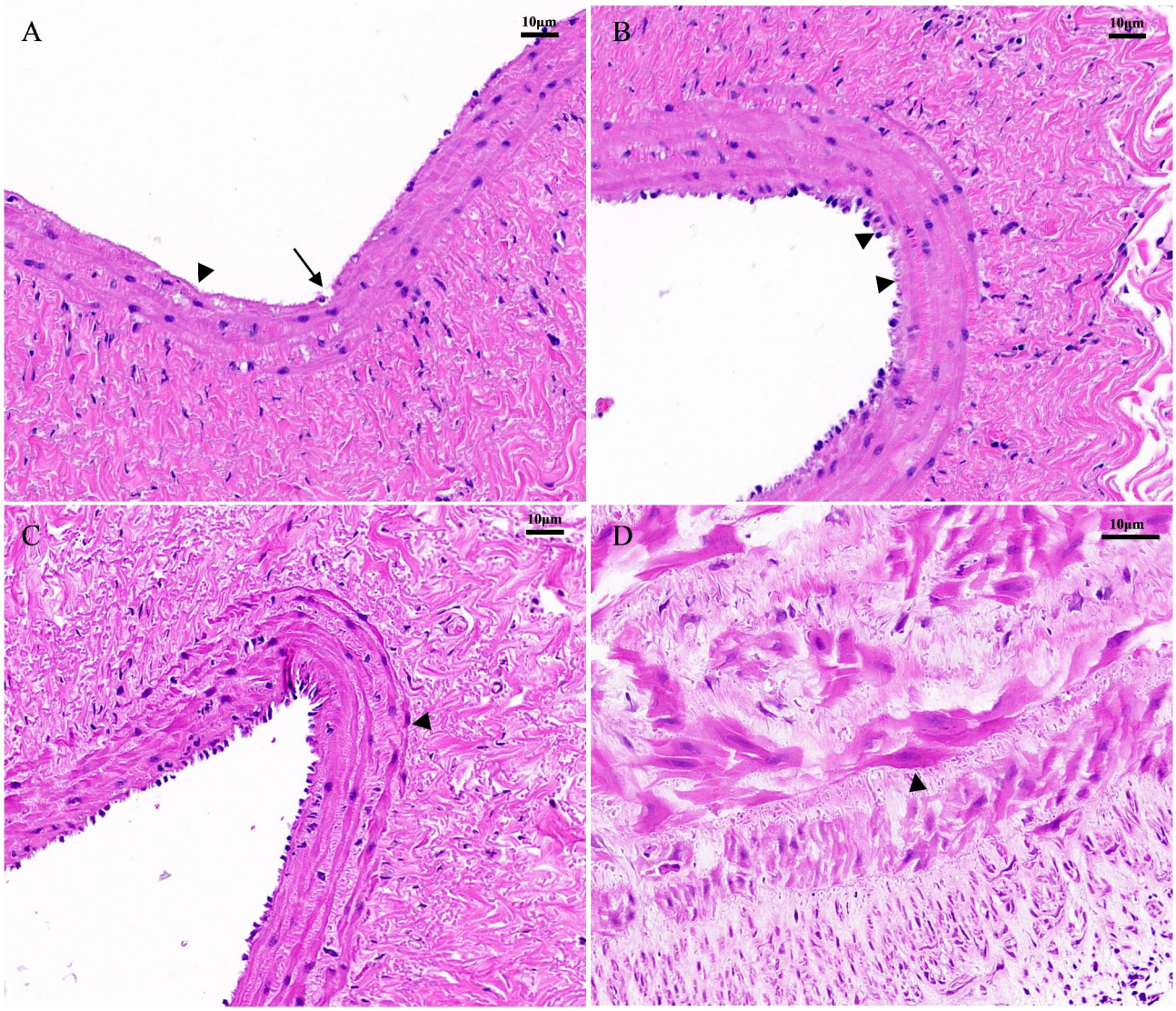

Fig. 6. CVC wall responses and VSMCs phenotypic transformation after IVC filter placement. (**A**) CVC wall injury (long arrow) and endothelial cell sloughing (short arrow) were observed after filter placement on H&E stain compared to normal CVC (**B**). (**C**,**D**) The migration and phenotypic transformation of VSMCs from a contractile type (**C**, short arrow) to a synthetic type (**D**, short arrow). Contractile VSMCs (**C**, short arrow) typically exhibit a stretched spindle shape. Synthetic VSMCs present a flattened fibroblast-like state with a significantly increased cell volume compared to the contracted phenotype of VSMCs (**D**, short arrow). *CVC* caudal vena cava, *VSMCs* vascular smooth muscle cells.

essentially identifying the optimal OR. This ensures the stability of the IVCF, prevents displacement, and reduces the risk of excessive intimal proliferation. To achieve this, designing diverse, personalized IVCF specifications is essential for the precise placement of IVCFs.

Limitations

Our study is subject to several limitations that merit consideration. Firstly, this model serves to stimulate vessel wall response for a general spindle-geometry filter, where the IVCF interacts directly with the CVC wall in a greater region and consequently the degree of IH would be greater[12]. The present model does not include other types of IVCFs such as umbrella-geometry filters. Furthermore, even for the IVCF design considerations in this study, vessel wall response has been simplified to the IVCF strut that is in contact with the CVC. Secondly, there is a lack of quantitative data on stress-strain levels known to cause vein injury. This study has not quantified the stress evolution induced by the IVCF struts that create the injury and consequently damage the wall and start the process. Thirdly, Chou et al.[18] found that damaged endothelial cells in blood vessels can recruit inflammatory cells and exacerbate vascular inflammation responses by releasing numerous inflammatory factors, triggering the proliferation and increased migration of VSMCs, thereby inducing phenotypic changes. However, the possible inflammatory response mechanisms were not elaborated. Fourthly, there is a limited number of swine,

and the hemodynamics analysis before and after IVCF placement was not incorporated in the present study. Fifthly, possible artifacts or distortions during the image reconstruction process may affect the precision of the diameter measurements. Paraffin-embedded sections undergo significant tissue shrinkage. The histological measurements are therefore far from any in vivo dimensions. In addition, the studies on receptors involved in cellular mechanosensing, exploring intracellular molecular and signaling pathway alterations, as well as more in-depth investigations at the genomic level, remain limited. Despite all the limitations and the lack of clinical results, this model can be considered a forward step to understanding IH proliferation under the influence of an IVCF with various diameters. Future studies should include the signaling pathway to better understand pathophysiology.

Conclusion

IH develops in response to CVC wall injury, VSMCs dedifferentiation, migration, proliferation, and secretion of the extracellular matrix of collagen fiber. RFs increased with the increased ORs of IVCF and CVC diameter. Increased ORs and dwelling time correlate linearly with greater IH and collagen fiber production. Moreover, RCS analysis revealed that ORs had a non-linear relationship with IH thickness and collagen fiber content after adjusting for the IVCF dwelling time.

Data availability

The datasets generated and analyzed during the current study are not publicly available, as the study data are related to other studies that are progressing but are available from the corresponding author upon reasonable request.

Received: 21 August 2024; Accepted: 29 January 2025
Published online: 25 March 2025

References

1. De Weese, M. S. & Hunter, D. C. Jr. A vena cava filter for the prevention of pulmonary emboli. *Bull. Soc. Int. Chir.* **17** (1), 17–25 (1958).
2. Kaufman, J. A. et al. Society of interventional radiology clinical practice guideline for inferior vena cava filters in the treatment of patients with venous thromboembolic disease: developed in collaboration with the American College of Cardiology, American College of Chest Physicians, American College of Surgeons Committee on Trauma, American Heart Association, Society for Vascular Surgery, and Society for Vascular Medicine. *J. Vasc. Interv. Radiol.* **31**, 1529–1544 (2020).
3. Kesselman, A. et al. Current controversies in inferior Vena Cava Filter Placement: AJR Expert Panel Narrative Review. *AJR Am. J. Roentgenol.* **216**, 563–569 (2021).
4. Sheahan, K. P., Tong, E. & Lee, M. J. A review of inferior vena cava filters. *Br. J. Radiol.* **96**(1141), 20211125 (2023).
5. Gong, M. et al. Incidence and risk factors for inferior vena cava filter thrombosis detected at time of filter retrieval in patients with lower extremity deep vein thrombosis: a multicenter retrospective cohort study. *Quant. Imaging Med. Surg.* **13**(12), 8313–8325 (2023).
6. Gong, M. et al. Characterization and risk factors of inferior vena cava thrombosis in situ detected by CT venography following filter placement: a single-center retrospective cohort study. *J. Vasc Surg. Venous Lymphat. Disord*. **12**, 101862 (2024).
7. Kuo, W. T. et al. Complex retrieval of embedded IVC filters: alternative techniques and histologic tissue analysis. *Cardiovasc. Interv. Radiol.* **35** (3), 588–597 (2012).
8. Thors, A. & Muck, P. Resorbable inferior vena cava filters: trial in an in-vivo porcine model. *J. Vasc. Interv. Radiol.* **22** (3), 330–335 (2011).
9. Dowell, J. D. et al. Celect inferior vena cava wall strut perforation begets additional strut perforation. *J. Vasc. Interv. Radiol.* **26** (10), 1510–1518 (2015).
10. Chen, L., Shi, W., Gu, J., He, X. & Lou, W. Atrophic inferior vena cava is a marker of chronicity of intra-filter and inferior vena cava thrombosis: based on CT findings. *BMC Cardiovasc. Disord*. **18** (1), 64 (2018).
11. Gong, M., Qian, C., Jiang, R., He, X. & Gu, J. Unveiling the link: minimum inferior vena cava diameter and thrombosis risk. *Acad. Radiol.* **S1076-6332** (24), 00122–00123 (2024).
12. Nicolás, M., Peña, E., Malvè, M. & Martínez, M. A. Mathematical modeling of the fibrosis process in the implantation of inferior vena cava filters. *J. Theor. Biol.* **387**, 228–240 (2015).
13. Xiao, Y. D., Zhang, Z. S. & Ma, C. Cavographic vs. cross-sectional measurement of the inferior vena cava diameter before filter placement: are we routinely oversizing? *Eur. Radiol.* **29**, 3281–3286 (2019).
14. Jensen, L. F., Bentzon, J. F. & Albarrán-Juárez, J. The phenotypic responses of vascular smooth muscle cells exposed to mechanical cues. *Cells* **10** (9), 2209 (2021).
15. Tang, Y. et al. MFN2 prevents neointimal hyperplasia in vein grafts via destabilizing PFK1. *Circ. Res.* **130** (11), e26–e43 (2022).
16. Chou, C. C., Wang, C. P., Chen, J. H. & Lin, H. H. Anti-atherosclerotic effect of hibiscus leaf polyphenols against tumor necrosis factor-alpha-induced abnormal vascular smooth muscle cell migration and proliferation. *Antioxidants (Basel)* **8** (12), 620 (2019).
17. Wang, Z. et al. Nuclear factor-κB is activated in filter-implanted vena cava. *Cardiovasc. Interv Radiol.* **42** (4), 601–607 (2019).
18. Macabrey, D. et al. Hydrogen sulphide release via the angiotensin converting enzyme inhibitor zofenopril prevents intimal hyperplasia in human vein segments and in a mouse model of carotid artery stenosis. *Eur. J. Vasc. Endovasc. Surg.* **63** (2), 336–346 (2022).

Author contributions

Conceptualization: MFG, RJ, XH, JPG; Data curation: MFG, RJ; Formal analysis: MFG, RJ; Funding acquisition: MFG; Investigation: MFG, RJ, XH, JPG; Methodology: MFG, XH, JPG; Project administration: JPG; Writing – original draft: MFG; Writing – review & editing: MFG, RJ, XH, JPG.

Funding

This work was supported by the Jiangsu Medical Association Special Fund Project [SYH-3201140-0088(2023035)], Nanjing Medical Science and Technology Development Project (YKK23116), "Vein Leading the Future" Venous

and Lymphatic Health Fund Project, and Nanjing Medical University Science and Technology Development Fund Project (NMUB20230163).

Declarations

Competing interests
The authors declare no competing interests.

Ethical approval and consent to participate
The study protocol was reviewed and approved by the institutional review board (IRB) of Nanjing First Hospital. The study is reported in accordance with ARRIVE guidelines (https://arriveguidelines.org).

Additional information
Supplementary Information The online version contains supplementary material available at https://doi.org/10.1038/s41598-025-88585-1.

Correspondence and requests for materials should be addressed to J.G.

Reprints and permissions information is available at www.nature.com/reprints.

Publisher's note Springer Nature remains neutral with regard to jurisdictional claims in published maps and institutional affiliations.